# An Experimental Adaptive Nulling Receiver Utilizing the Sample Matrix Inversion Algorithm with Channel Equalization

J. Russell Johnson, Alan J. Fenn, *Senior Member, IEEE*, Herbert M. Aumann, *Member, IEEE*, and Frank G. Willwerth

*Abstract*—**The suppression of external interference in an adaptive radar is often limited by frequency-dependent channel tracking errors. Techniques for effectively equalizing a narrow-band side-lobe canceler are discussed in this paper, and an experimental four-channel receiver that supports both open-loop and closed-loop operation is described. As implemented, three different canceler modes are possible: feedforward, feedback, and a tandem feedback/feedforward combination. All three modes have been successfully demonstrated in bench experiments with a broad-band noise source using the sample matrix inversion algorithm.**

## I. Introduction

FUTURE radar systems may be confronted with strong resistance in the form of noise jamming through the radar antenna's side lobes. Low side lobes and spread spectrum techniques may reduce the impact of noise jamming, but adaptive nulling is the radar's most effective defense. With advances in high-speed digital signal processing technology, the sample matrix inversion (SMI) method [1] may soon become economically feasible in a number of applications. Although the SMI algorithm enjoys well-known theoretical advantages with regard to convergence, actual performance has been found to be sensitive to receiver channel tracking errors [2]. This paper explores two ideas for effectively achieving channel equalization within the framework of a narrow-band side-lobe canceler. The first approach relies primarily on digital equalization to enhance conventional SMI performance, whereas the second utilizes feedback to extend the SMI method into the realm of analog adaptive cancellation. The latter approach may ease some digital signal processing requirements, although not without increasing the complexity of the receiver. In demanding applications, further improvements in nulling performance may be realized by combining feedback and feedforward cancellers in *tandem*. Cancellation ratios in excess of 50 dB have been achieved in a four-channel test-bed system.

The organization of this paper is as follows: Section II introduces a general receiver architecture for reducing channel mismatch effects. Three modes of operation are incorporated in this architecture: all-digital feedforward, hybrid feedback, and a tandem combination of feedforward/feedback techniques. Each mode of operation is described and the basic algorithms for channel equalization and adaptive weight updating are discussed. A four-channel experimental receiver with the multimode architecture is described in Section III. A novel arrangement of attenuation and phase control devices is used to achieve adaptive weighting of the receiver channels. A brief description of the nulling receiver is given along with pertinent measured data for the narrow-band filters as well as the adaptive weights. Receiver channel tracking and digital equalization performance are examined in Section IV. The results of adaptive cancellation bench tests are presented in Section V and our conclusons are summarized in Section VI.

## II. Multimode Adaptive Nulling Architecture

Three side-lobe canceler configurations have been investigated with the demonstration system described in the following section. The SMI algorithm is employed in all three architectures and in each case some form of digital equalization is utilized. The basic open-loop configuration is referred to here as the all-digital feedforward mode. In this case, the receiver channels are equalized digitally and an adaptive null is formed in the digital domain. In the closed-loop configurations, the signals in each channel are phase/amplitude weighted and then combined to form an analog null. Since the analog weights are actually controlled digitally, the basic closed-loop configuration is called the hybrid feedback mode. In the tandem mode, the outputs of the hybrid feedback canceler serve as inputs for a conventional (digital) SMI canceler. The three cancellation modes are depicted in Fig. 1 and are further explained below. For simplicity, only a single representative auxiliary channel is shown for each mode.

Manuscript received August 20, 1990; revised December 4, 1990. This work was supported by the Department of the Air Force under Contract F19628-90-C-0002.

The authors are with Lincoln Laboratory, Massachusetts Institute of Technology, Lexington, MA 02173-9108.

IEEE Log Number 9143005.

0018-9480/91/0500-0798$01.00 ©1991 IEEE

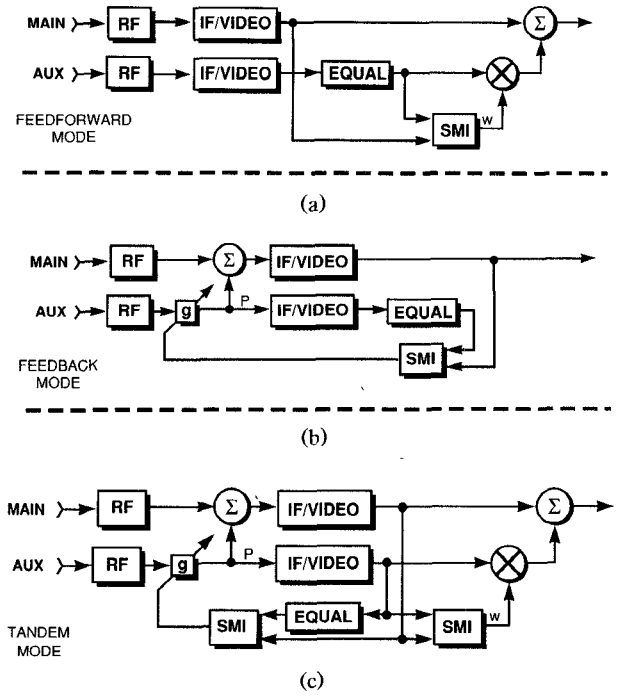


Fig. 1. Adaptive nulling receiver modes of operation implementing the sample matrix inversion algorithm with channel equalization: (a) feedforward mode; (b) feedback mode; and (c) tandem mode.

### *A. Modes of Operation*

In the all-digital feedforward mode (Fig. 1(a)), an equalization filter is implemented digitally for each receiver channel. The main channel serves as a convenient reference and the auxiliary channels are equalized with respect to this reference. Analog tapped delay lines traditionally serve as adaptive equalizers in wide-band nulling systems, and the digital equivalent is referred to here as a finite impulse response (FIR) equalizer. Filter coefficients for a FIR equalizer are readily determined using least squares methods [3]. Equalizer coefficients and adaptive nulling weights are best determined separately in narrow-band applications. This requires an independent calibration procedure for adjusting the equalizers, but the additional effort is generally worthwhile since the computation rate for determining the adaptive (SMI) weights is reduced considerably. Satisfactory results have been obtained using either broad-band noise or a stepped CW signal as a calibration source.

Adaptive weights in side-lobe cancelers have traditionally been implemented with analog circuitry [4]. Most analog feedback techniques are based on the method of steepest descent, and the rate of adaptation is highly dependent on system implementation details as well as the interference environment. In contrast, the convergence properties of the SMI method are completely determined by the number of receiver channels and the number of statistically independent samples used to estimate the theoretical covariance matrix or its "voltage-domain" equivalent. In principle, the convergence properties of the SMI algorithm can be exploited by the hybrid feedback scheme in Fig. 1(b) to obtain an essentially optimum nulling solution almost instantly. An analog null is produced in the receiver by adjusting a digitally controlled, complex weight in each channel and then coherently combining the weighted signals.

Simulation studies [5] suggest that the hybrid feedback technique can be effectively applied in narrow-band systems provided channel tracking errors in the receiver are carefully controlled or, if necessary, compensated by the digital signal processor. In our experimental work, certain complications that may arise in attempting to equalize an adaptive receiver have been avoided by placing the analog weight in each (auxiliary) channel before the power divider or *pickoff point* (denoted by the letter $P$ in Fig. 1(b)). This architecture departs from the conventional arrangement found in the Howells-Applebaum loop [6], [7], where adaptive weighting occurs after the pickoff point. The analog weights were implemented with voltage-variable attenuators and phase shifters controlled by 16 b D/A (digital to analog) converters. D/A quantization errors are negligible and the aforementioned architecture reduces the impact of calibration errors.

An all-digital adaptive nulling solution is clearly desirable whenever rapid convergence is paramount. However, the potential for greatly improved cancellation provided by digital equalization places a large premium on receiver linearity and dynamic range. In this respect, A/D (analog to digital) converters have obvious limitations. When dynamic range is the primary issue, the hybrid feedback technique offers a significant advantage, namely, a substantially reduced output power level. Controlled by an SMI processor, the convergence of the feedback mode is not governed by covariance matrix eigenvalue spread as discussed in [7]. Nevertheless, the ambivalent behavior of underdetermined SMI weights can sometimes hinder adaptation. Although excessive weight jitter can be controlled by diagonally loading the sample covariance matrix, the response of the feedback mode may occasionally be slower than one might like. In such instances, the tandem nulling technique [8] shown in Fig. 1(c) generally hastens convergence. Ostensibly, the second (digital) stage of cancellation corrects small errors that may limit analog nulling performance.

### *B. Equalization*

Even with careful receiver design, channel equalization may be necessary in order to achieve good cancellation performance. The two signal processing techniques discussed below are specifically aimed at determining filter coefficients for an FIR equalizer. The deterministic method is based on the receiver's response to a sequence of CW signals spanning the equalization bandwidth. Alternatively, a receiver can be equalized adaptively on the basis of its response to an external source of broad-band noise (e.g., a jammer). The adaptive approach is perhaps easier to implement whereas the deterministic approach is potentially more accurate. The least squares principle

provides a solid mathematical foundation for both. In the extended least squares algorithm described below, the output of a receiver channel is represented as a complex signal matrix. In turn, the equalization techniques are completely characterized by the procedures used to generate the signal matrices. In the experimental system, an $M \times N$ signal matrix is constructed for each channel from calibration data as described below.

In general, the equalization objective is to determine the best possible digital filter with a finite impulse response described by $N$ complex coefficients. The adaptive method is described first since the preliminary signal processing is minimal. In this case, a wide-band noise source is applied to the receiver inputs and data are recorded at the outputs of the appropriate channels. Assuming $N$ equalizer coefficients suffice, I/Q (in-phase/quadrature) data are arranged in rows made up of $N$ contiguous samples. Theoretical results [9] based on the complex Wishart distribution suggests that $M = 5N$ statistically independent rows should yield nearly optimum performance for an $N$-tap equalizer.

In a side-lobe canceler, the main channel provides a natural reference for equalizing the auxiliary channels. Since the auxiliaries are treated identically, it suffices to consider only one for this discussion. Thus, let $\boldsymbol{X}$ and $\boldsymbol{Y}$ be $M \times N$ signal matrices for the auxiliary and main channels, respectively, constructed in the manner described above. Using matrix multiplication, the equalizer output can be represented as $\boldsymbol{Xw}$, where $\boldsymbol{w}$ is a column vector of reversed FIR coefficients

$$w_n = h_{N-n}, \qquad n = 1, \cdots, N \tag{1}$$

chosen to make the filter output match the reference signal as closely as possible. Strictly speaking, the auxiliary channel is equalized with respect to the main channel by taking the rightmost column of $\boldsymbol{Y}$ as the target. However, better performance is generally obtained by introducing a delay in the reference channel. The remaining columns of $\boldsymbol{Y}$ taken in reverse order (i.e., from right to left) represent a sequence of cases where the equalization delay increases from one to $N-1$ sampling intervals. Filter coefficients for all $N$ cases are given by the matrix $\boldsymbol{W}$ that minimizes

$$\boldsymbol{E} = \boldsymbol{Y} - \boldsymbol{XW} \tag{2}$$

in the usual least squares sense. The residual channel tracking error is given, as a function of equalization delay, by the main diagonal elements of the residual covariance $\boldsymbol{E}^H\boldsymbol{E}$, where $^H$ represents the conjugate (Hermitian) transpose operator. The best equalization performance is obtained by identifying the filter coefficients with the column of $\boldsymbol{W}$ corresponding to the smallest diagonal element of $\boldsymbol{E}^H\boldsymbol{E}$. The least squares solution is easily derived from the extended matrix $\boldsymbol{Z} = [\boldsymbol{X} \quad \boldsymbol{Y}]$. The $QR$ decomposition of $\boldsymbol{Z}$, where $\boldsymbol{Q}$ is a unitary matrix and $\boldsymbol{R}$ is an upper (right) triangular matrix, or, equivalently, the Cholesky factorization [10]

$$\boldsymbol{Z}^H\boldsymbol{Z} = \begin{bmatrix} \boldsymbol{X}^H\boldsymbol{X} & \boldsymbol{X}^H\boldsymbol{Y} \\ \boldsymbol{Y}^H\boldsymbol{X} & \boldsymbol{Y}^H\boldsymbol{Y} \end{bmatrix} = \boldsymbol{R}^H\boldsymbol{R} \tag{3}$$

then leads directly to the desired solution. Partitioning $\boldsymbol{R}$ along similar lines, we have

$$\boldsymbol{R} = \begin{bmatrix} \boldsymbol{U} & \boldsymbol{V} \\ \boldsymbol{0} & \boldsymbol{T} \end{bmatrix} \tag{4}$$

where $\boldsymbol{U}$ and $\boldsymbol{T}$ are also upper triangular matrices. It can be shown that the least squares solution is given by $\boldsymbol{W} = \boldsymbol{U}^{-1}\boldsymbol{V}$ and that $\boldsymbol{T}$ is the Cholesky triangle of the residual covariance (i.e., $\boldsymbol{E}^H\boldsymbol{E} = \boldsymbol{T}^H\boldsymbol{T}$). Consequently, the residual channel tracking errors

$$|E_{nn}|^2 = \sum_{m=1}^{n} |T_{mn}|^2 \tag{5}$$

can be easily computed without having to first solve $\boldsymbol{UW} = \boldsymbol{V}$ for the filter coefficients. The residual channel tracking error may actually be fairly insensitive to the equalization delay, and in these instances utilizing a different delay for each auxiliary channel would be a nuisance. Needless complications can be avoided by choosing the equalization delay to minimize the worst-case channel tracking error.

Using broad-band noise for a calibration source has the potential disadvantage that A/D converter saturation generally becomes intolerable at a significantly lower average power level than with CW signals. Thus, one might reasonably expect traditional calibration techniques to yield better equalization performance. In the demonstration system described in the following section, equalizer coefficients are computed on the basis of $M = 85$ calibration frequencies.

To apply the least squares principle in the frequency domain, at a finite number of points $\{f_m | m = 1, \cdots, M\}$, the canonical form of a signal matrix is

$$X_{mn} = X(f_m)D^{-n}(f_m) \tag{6}$$

where $X(f)$ denotes the channel frequency response and

$$D(f) = \exp\{-j2\pi f\Delta t\} \tag{7}$$

is the Fourier transform normally associated with a time delay equal to the sampling interval $\Delta t$. In this case, the distribution of the residual channel tracking error over the equalization bandwidth can be controlled to some degree by preweighting the signal matrices. This refinement would perhaps be appropriate for applications in which the interference exhibits a (known) nonuniform power spectral density.

The calibration frequencies and the sampling interval must be known explicitly in order to apply (7) in (6). In practice, it may be easier or more reliable to determine $D(f_m)$ directly from calibration data using a straightforward correlation technique. Thus, let $x_m(k)$ denote the $k$th I/Q (i.e., complex) sample obtained from the $m$th calibration record. Each record represents the noise-corrupted response of a particular receiver channel to a CW

calibration signal with some fixed but possibly unknown frequency. If the calibration SNR is very large, additional signal processing may be unnecessary; i.e., simply identifying $X_{mn}$ with $x_m(n)$ may suffice. Otherwise, we proceed by first calculating

$$C_m = \sum_{k=1}^{K} x_m(k)\, x_m^*(k-1) \tag{8}$$

where * is the complex conjugate operator. Setting

$$D(f_m) = |C_m| / C_m \tag{9}$$

effectively estimates the product $f_m \Delta t$ and the channel frequency response is subsequently obtained by correlating the I/Q data with $D^{-k}(f_m)$. The result of this operation may be expressed as

$$X(f_m) = \sum_{k=0}^{K} x_m(k) D^k(f_m) \tag{10}$$

since the identity $D^{-1} \equiv D^*$ clearly holds for (9).

The feedback rules discussed in the following section assume that the adaptive receiver is properly equalized. Generally speaking, equalizer coefficients derived from open-loop calibration procedures are not directly applicable to the closed-loop modes. For closed-loop operation, the inputs to all but one channel are disabled and equalizer coefficients for the remaining channel are derived using the output of the closed-loop main channel as a reference. The result is that the two paths from the pickoff point to the adaptive processor (see Fig. 1b) have essentially the same frequency response. The process is repeated for each channel.

### C. Adaptive Weight Updating

The receiver architecture in Fig. 1(b) is referred to here as a preweighting canceler. The distinguishing feature of this type of canceler is that the adaptive weight occurs *before* the pickoff (sampling) point $P$. This unorthodox arrangement evolved from a rather innovative method of implementing adaptive weights. In the experimental receiver, attenuation occurs in the first IF (intermediate frequency) stage while the phase shift is applied in the LO (local oscillator) line driving the IF mixer. This implementation simplifies the calibration task significantly, since the amplitude dependence of the phase shifters is effectively eliminated. The first IF stage was implemented at 200 MHz, and the measured variation of the attenuators' frequency response was negligible over the 1 MHz nulling bandwidth. Consequently, the adaptive weights in the experimental receiver are essentially frequency independent. However, the standard algorithm for adjusting adaptive weights must be revised in order to accommodate a preweighting canceler. It will be shown that the required modification turns out to be ideally suited for the class of adaptive weights which precipitated the new architecture.

In the testbed receiver, the main channel depends on the mode of operation. For closed-loop operation, the primary open-loop input is discarded and the output of the analog combiner becomes the primary closed-loop input. This arrangement economizes on channels and is adequate for the bench tests described in Section IV. However, for the purpose of discussion, let us suppose that the open-loop main channel is retained as an alternative primary input. The closed-loop main channel provides the adapted main-beam signal, generated within the receiver, while the open-loop main channel carries the unadapted or quiescent main-beam signal. The latter is the primary input to the all-digital feedforward canceler, while the closed-loop main channel supplies the primary input to the tandem canceler. The role of the open-loop main channel in the closed-loop modes is discussed below.

With the two main channels postulated above, "open-loop feedback" is a distinct possibility. The interpretation of this apparent misnomer is that the analog weights are adjusted on the basis of SMI weights calculated for the all-digital feedforward mode. A similar open-loop technique was previously utilized [11] in a master/slave arrangement, and at least a modicum of success was achieved without digital equalization. In our application, open-loop feedback could be utilized to initialize or, if warranted, reinitialize the analog weights. It should be emphasised, however, that the update rules for open-loop and closed-loop feedback are not the same.

The method of computing FIR equalizer weights discussed in the previous section can be used to calculate SMI weights for a side-lobe canceler by reinterpreting the signal matrices $X$ and $Y$ appropriately. In this case, each row of $X$ ($Y$) represents an independent "snapshot" of the outputs of the auxiliary (main) channels. Evidently, the extended triangularization implicit in (4) is directly applicable to receivers with multiple output channels. In particular, an estimate of the noise residue for each mode of the experimental receiver is readily available from (5). Consequently, the adaptive processor can first determine the cancellation performance achieved in each mode and then compute the weights for the preferred mode. Let

$$m = \begin{cases} 0; & \text{open-loop} \\ 1; & \text{closed-loop} \end{cases} \tag{11}$$

indicate the main channel selected by the adaptive processor. The digital weight $w$ for an arbitrary channel calculated by the adaptive (SMI) processor generally depends on $m$. Moreover, the feedback rule for updating the corresponding analog weight, say $g$, also depends on $m$. In a conventional canceler, $g = w$ if $m = 0$ (open-loop feedback) whereas $\Delta g = w$ if $m = 1$ (closed-loop feedback). For a preweighting canceler, the update rules are given by $\Delta g = (m - 1 + w)g$, or equivalently, $g \leftarrow (m + w)g$, where the arrow signifies replacement.

In the testbed receiver, the adaptive weight in each channel is functionally equivalent to an attenuator and a phaser placed in series. This type of weight is controlled in a logarithmic manner; thus its complex voltage gain

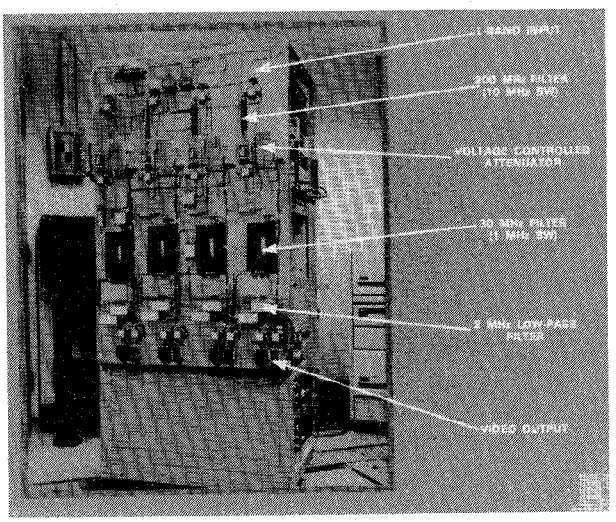

(a)

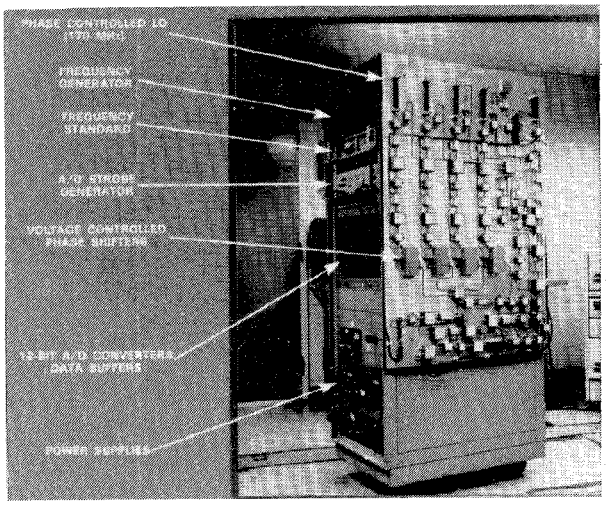

(b)

Fig. 2. Integrated adaptive nulling testbed. (a) Left side view. (b) Right side view.

(value) is naturally represented as $g = e^z$, where the real and imaginary components of $z = \alpha + j\phi$ specify the attenuation and the phase shift, respectively. When logarithmic weights are implemented in a preweighting canceler, the update rules can be expressed as

$$\Delta z = \log(m + w) \tag{12}$$

which is independent of $z$. On the other hand, if logarithmic weights are utilized in a conventional canceler, $\Delta z = \log(m + we^{-z})$ clearly depends on the current value of the analog weight.

## III. Demonstration System

This section describes an experimental L-band adaptive nulling system. Photographs of the four-channel receiver are shown in Fig. 2 and its relevant design parameters are listed in Table 1. A block diagram of the testbed configuration is depicted in Fig. 3. A more detailed diagram of a representative channel is shown in Fig. 4.

TABLE I
Adaptive Nulling Receiver Testbed Parameters

| | |
|---|---|
| Number of Channels | 4 |
| Frequency Range | 1.25 to 1.35 GHz |
| Instantaneous Bandwidth | 1 MHz |
| A/D Converters | 12-b, 5 MHz |
| Nulling Weights (IF) | 16-b Amp./Phase |
| First IF | 200 MHz |
| Second IF | 30 MHz |
| Baseband Offset | 1.5 MHz |

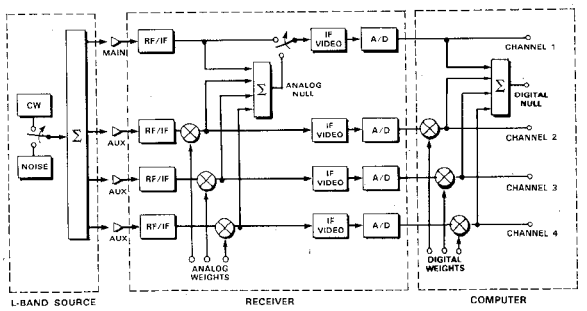


Fig. 3. Four-channel adaptive nulling receiver configuration.

The RF front end serves to amplify, filter, and down-convert the L-band signal to the first IF of 200 MHz. By varying the first LO frequency, the receiver can be tuned over a 100 MHz band, from 1.25 to 1.35 GHz. After down-conversion to the first IF frequency of 200 MHz, the signal is filtered with a 10 MHz bandwidth filter. Up to 40 dB of adaptive attenuation can be applied at this point. The signal is then mixed to the second IF of 30 MHz with an adaptively phase-controlled 170 MHz LO. Prior to narrow-band filtering, the 30 MHz signal is coupled off to an analog nulling junction. Several computer-controlled switches permit arbitrary selection or termination of the signals going to the nulling junction. A third mixing process with a 28.5 MHz LO brings the signal down to baseband with a 1.5 MHz frequency offset. The baseband signal is subsequently digitized by a 12 b A/D converter at a 4.5 MHz sampling rate. With appropriate low-pass and digital I/Q filtering, the offset frequency avoids image and bias problems and minimizes harmonic distortion introduced by the video amplifiers.

In the experimental system, data collection and processing are carried out in a batch mode. Under computer control, an RF signal is injected into the front end of the four receiver channels via a power divider. The computer then triggers a programmable pulse generator which sends out a burst of 256 pulses to all four A/D converters. The same set of pulses is also used to strobe A/D data into four data buffers. After the buffers are full, the computer sequentially addresses each buffer and transfers the data to memory for further processing. A complex (I/Q) representation of the received signal is generated from the A/D data using a 47-tap FIR filter derived from a Dolph–Chebyshev window function. The frequency response of this filter is shown in Fig. 5. The digital architecture depicted in Fig. 6 intrinsically down-samples the

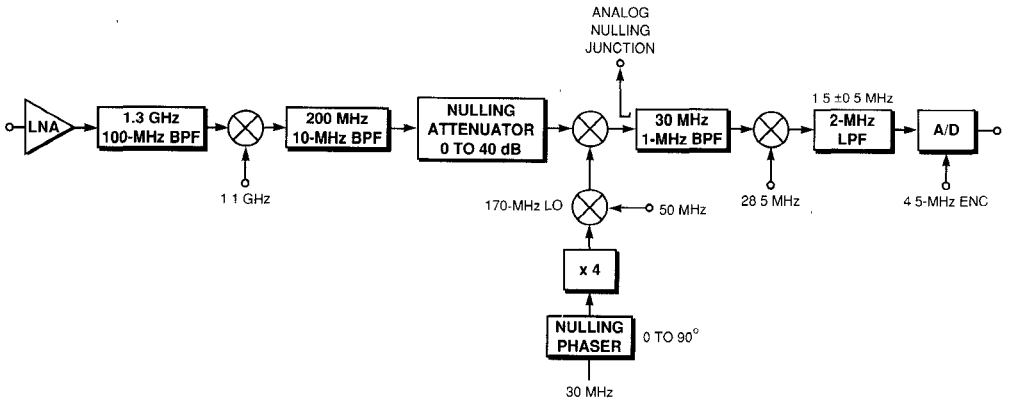


Fig. 4. Block diagram for one channel of the adaptive nulling receiver. Nulling amplitude weights are applied at 200 MHz and nulling phase weights are applied in the 170 MHz LO. Narrow-band filtering occurs after the nulling weights are applied.

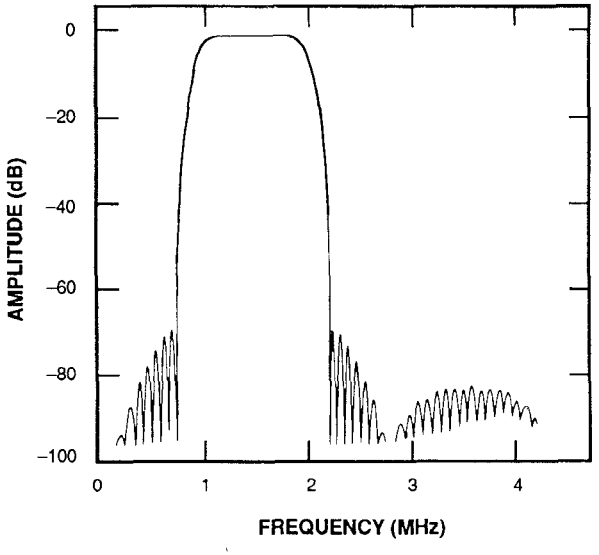


Fig. 5. I/Q filter frequency response.

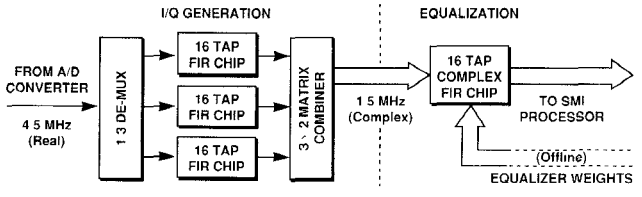


Fig. 6. Digital filter architecture for I/Q generation and channel equalization.

I/Q filter output by 3:1 before applying it to the FIR equalizer. In the demonstration system, I/Q filtering and channel equalization were actually implemented with software.

The 1 MHz instantaneous receiver bandwidth is established in the second IF (30 MHz) stage by six-section cavity filters. The effective frequency response of the four narrow-band filters, as viewed at baseband, is shown in Fig. 7. The differences in the frequency responses of all four cavity filters (relative to the average) are shown in Fig. 8. If uncompensated, these amplitude and phase

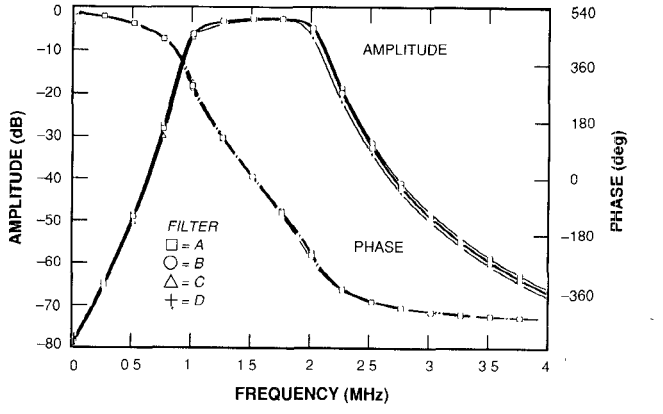


Fig. 7. Measured frequency response for the four 30 MHz IF band-pass filters as viewed over the down-converted (baseband) frequency range.

(tracking) errors would limit cancellation between any two channels to 25 dB or less.

Voltage-variable attenuators and phasers controlled by 16 b D/A converters were used to implement the analog nulling weights. Fig. 9 shows the measured response of the auxiliary channels as a function of the normalized D/A inputs. As indicated in Fig. 9(a), the attenuators provide monotonic amplitude control over a 40 dB dynamic range. The nonlinear input/output relationship is easily calibrated digitally. Fig. 9(b) shows a significant phase shift associated with a change in attenuation which must also be taken into account when setting the adaptive weights. In order to obtain the nearly linear phaser response shown in Fig. 9(c), a maximum phase shift of 90° is applied to a 30 MHz LO signal. The fourth harmonic of the phase-shifted signal is selected and then mixed with a 50 MHz LO signal to generate a 170 MHz LO signal with 360° of phase control.

The task of setting the adaptive weights is generally complicated by phase errors in the attenuators. However, amplitude errors that might otherwise be caused by the phasers are virtually eliminated by introducing the phase shift in a mixer under nearly saturated conditions. Consequently, the adaptive weights in the testbed receiver can

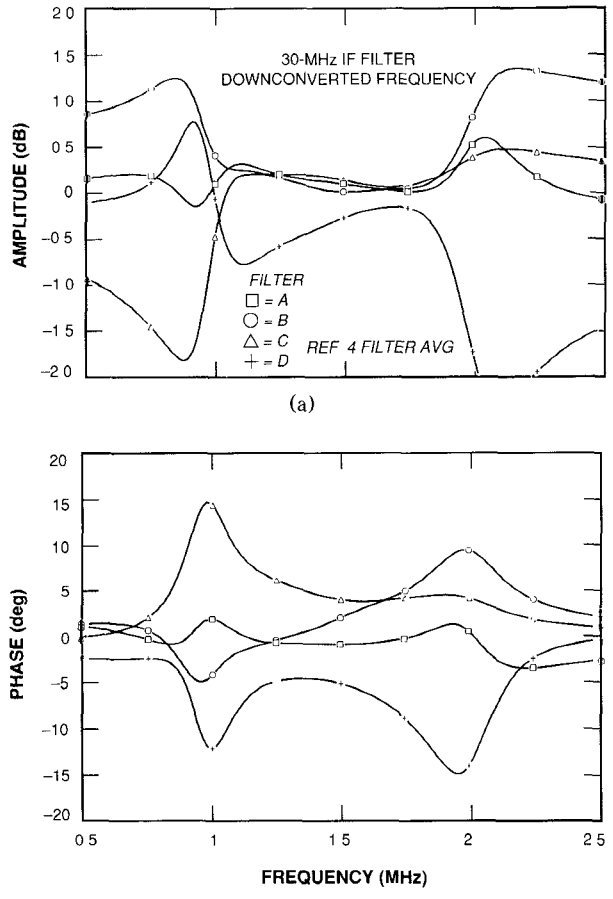


Fig. 8. Measured frequency response differences (relative to the average) for the 30 MHz IF band-pass filters as viewed over the down-converted (baseband) frequency range: (a) amplitude and (b) phase.

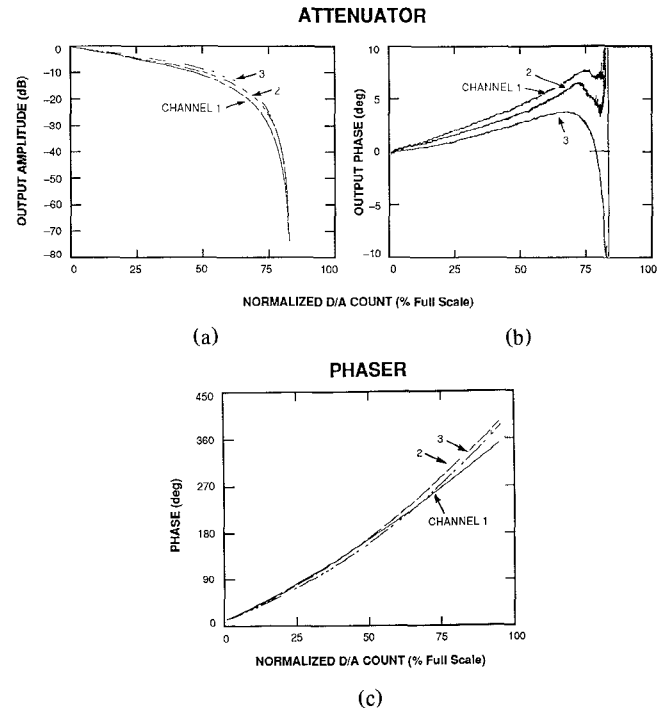


Fig. 9. Measured response of adaptive nulling weights as a function of D/A converter input: (a) attenuator amplitude response; (b) attenuator phase error; and (c) phaser phase response.

be controlled very accurately by first setting the attenuators and determining the resulting phase errors from calibration data; the phaser settings are then adjusted accordingly.

## IV. Receiver Channel Tracking

The channel mismatch (frequency response differences) for the all-digital feedforward mode is shown in Fig. 10. Similarly, Fig. 11 shows the relevant channel mismatch for the hybrid feedback mode. Notice that the errors are almost exactly the same in the two cases. The similarity is due to the fact that all components preceding the analog nulling junction are relatively wide-band compared with the narrow-band cavity filters. The last point is important, since the hybrid feedback technique cannot compensate channel tracking errors that occur before (outside) the feedback loop. In the experimental receiver, the analog null is formed prior to the narrow-band filter in the main channel, and the pickoff points precede the narrow-band filters in the auxiliary channels.

FIR equalizer coefficients are extracted from calibration data as described in Section II. A testbed calibration procedure typically produces 128 blocks of CW data covering the entire baseband from dc to 2.25 MHz. Each block contains the receiver's response to a different CW frequency, and since the bandwidth of the equalizers is limited to 1.5 MHz, only the 85 blocks spanning 0.75–2.25 MHz are used for equalization purposes. Receiver channel tracking performance is shown in Fig. 12 as a function of the number of taps (filter coefficients) permitted in the equalizer. The results indicate that 16 taps should suffice for achieving 50 dB cancellation in the experimental system. Without equalization, the channel tracking error normally varies between $-30$ dB and $-20$ dB. As discussed above, these errors are almost entirely attributable to the narrow-band cavity filters.

The frequency response of the four receiver channels, before and after equalization, is shown in Fig. 13 for the feedforward mode. The elimination of both the negative frequency image and the spurious dc component by the I/Q filter is clearly evident in Fig. 13(b).

## V. Cancellation Ratio Tests

The three modes of operation described in Section II have been investigated in a series of bench tests. For these tests, wide-band noise was injected into the receiver channels through a four-way power divider and coaxial cables. The cable lengths are matched for calibration purposes and during "nondispersive" tests. In "dispersive" tests, cables of different lengths are substituted (after calibration) in order to simulate the effect of a jammer wavefront arriving at slightly different times at each of four antenna receiving elements.

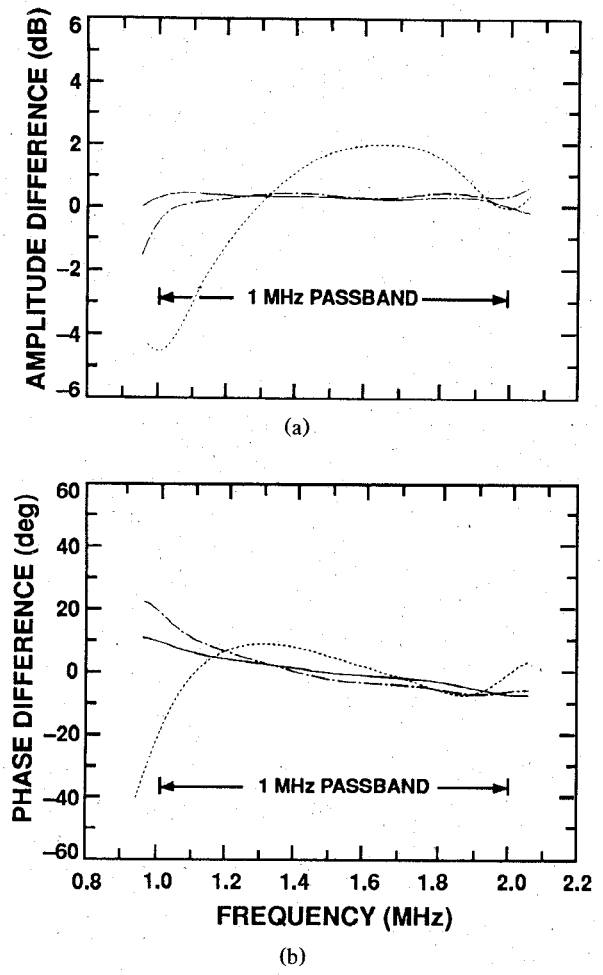


Fig. 10. Measured RF to baseband auxiliary-channel mismatch (relative to open-loop main channel) for the all-digital nulling case: (a) amplitude and (b) phase.

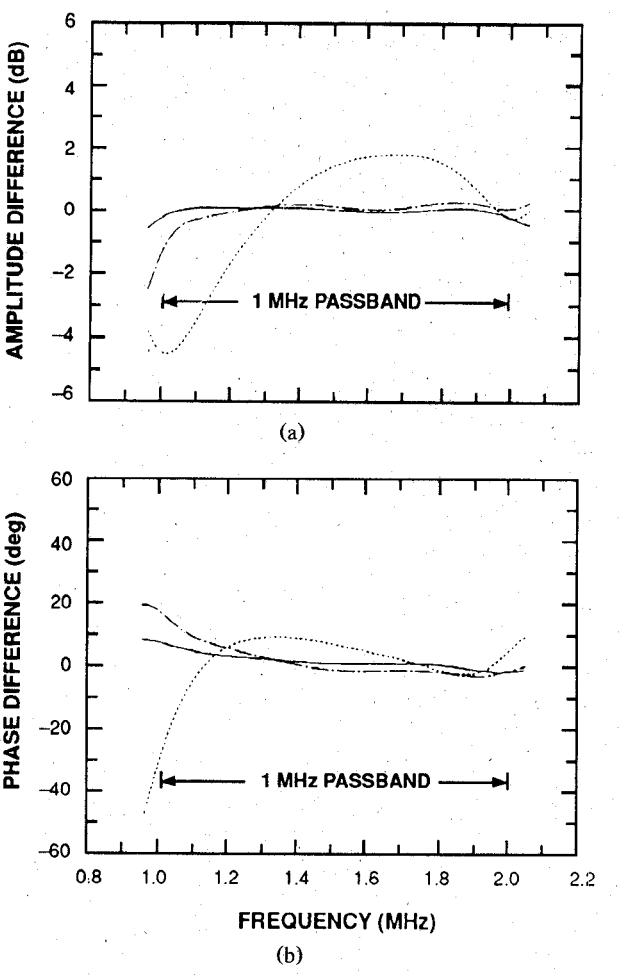


Fig. 11. Measured IF to baseband auxiliary-channel mismatch (relative to closed-loop main channel) for the hybrid-feedback case: (a) amplitude and (b) phase.

Experimental results obtained from both dispersive and nondispersive tests are shown in Fig. 14 for the all-digital feedforward mode. Before adaptation, the jammer power at the output of the receiver main channel is about 53 dBq, where q signifies the quantization level (i.e., least significant bit) of the A/D converter. With a sufficient number of auxiliary channels (i.e., degrees of freedom) and 16-tap equalizers, the interference level can be reduced to about 3 dBq for a cancellation ratio of 50 dB. Without equalization, cancellation performance degrades significantly, particularly if only one auxiliary channel is available. Under the mildly dispersive conditions simulated in these tests, two equalized auxiliary channels suffice for achieving the 50 dB cancellation objective.

Examples of the cancellation performance of all three modes are shown in Figs. 15 to 17. The two traces are the measured power levels at the input and output of the digital combiner. The experimental system does not operate in real time, and thus the power measurements have simply been plotted versus an iteration index. A block of 250 contiguous samples is collected and processed for each iteration. Iterations 1–59 establish the thermal noise level under quiescent conditions; the external interference is switched on at iteration 60. In Fig. 16 and 17, feedback is enabled at iteration 120.

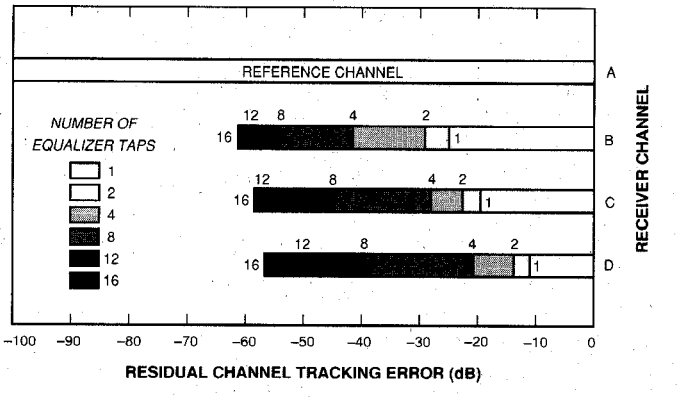


Fig. 12. Measured FIR equalization performance in terms of residual channel tracking error when the number of equalizer taps is varied from 1 to 16 for the four-channel adaptive nulling receiver.

Fig. 15 shows a typical dispersive test of the feedforward mode with three auxiliary channels. In the feedforward mode, the receiver gain is normally adjusted so that the quiescent (thermal) noise power is well below 0 dBq. This maximizes the useful dynamic range of the A/D

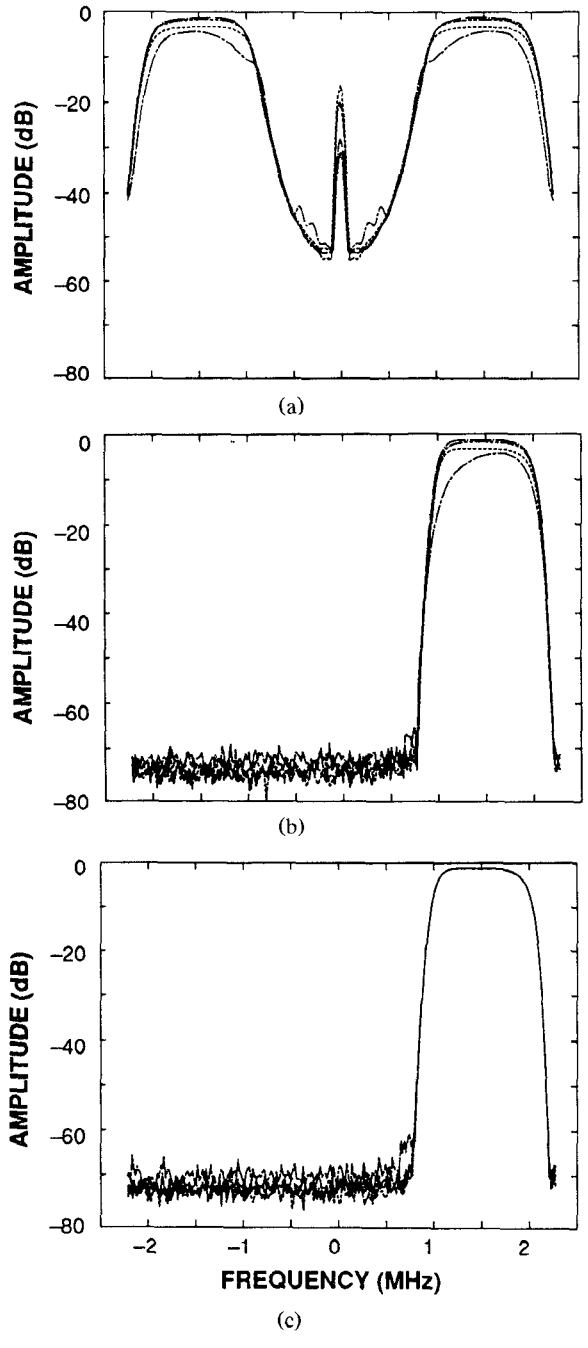


Fig. 13. Measured frequency response of the four-channel testbed receiver: (a) before I/Q filtering; (b) after I/Q filtering; and (c) after equalization.

converter for adaptive nulling purposes but adversely affects the noise floor of the system. Evidently, the residual interference level (after adaptation) in Fig. 15 is about 10 dB above thermal. A large increase in the effective system noise figure would be undesirable in a surveillance radar, for example, and under these circumstances the hybrid feedback method offers significantly improved performance. Fig. 16 demonstrates cancellation in the feedback mode over a larger dynamic range than is currently possible in the feedforward mode. When extra degrees of freedom are available, excessive weight jitter may affect the performance of the feedback mode, as seen in Fig. 17.

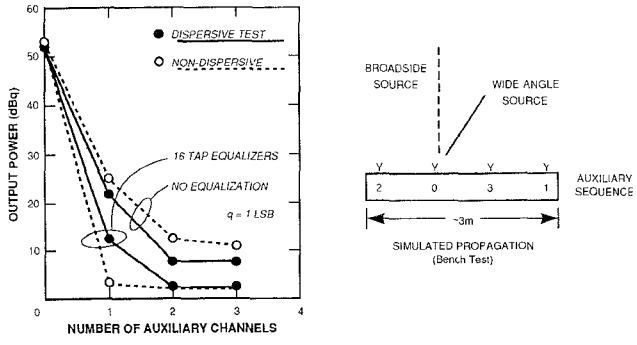


Fig. 14. Measured adaptive cancellation of one large jammer (with and without dispersion) as a function of the number of auxiliaries with the four-channel nulling receiver operating in the feedforward mode. A significant improvement in cancellation is evident when two or more auxiliary channels are used, as well as when equalizers with 16 taps are implemented.

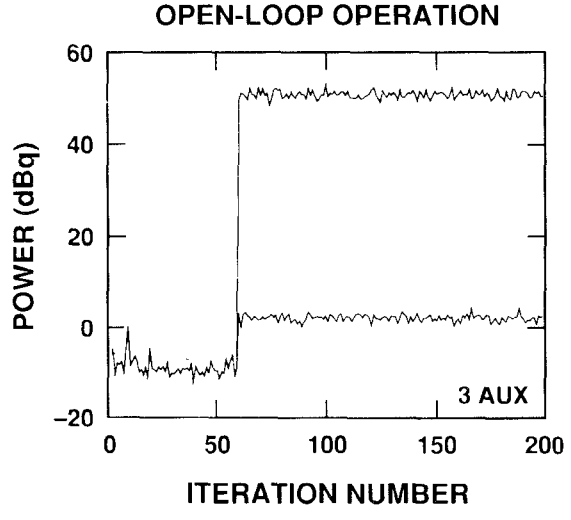


Fig. 15. Measured adaptive cancellation of one large jammer with the four-channel nulling receiver operating in the feedforward mode. The quiescent noise power (prior to iteration number 60) is well below 0 dBq. After adaptation the residual interference level is significantly above thermal noise which represents a degraded system noise figure.

In this nondispersive test case, the accelerated response of the tandem mode is apparent. In the closed-loop mode(s), the empirical cancellation ratio is 55 dB, and a null depth (i.e., the power ratio of the *external* interference before and after adaptation) of 58 dB at the canceler output can be inferred from the observed power levels.

## VI. Conclusion

An experimental receiver has been built in order to investigate promising new adaptive nulling concepts. Bench tests have demonstrated that the SMI method is capable of significantly better cancellation when augmented with digital equalizers. The measured results presented in this paper clearly establish the importance of channel equalization as well as the need for adequate adaptive degrees of freedom when confronted with dispersive jamming signals.

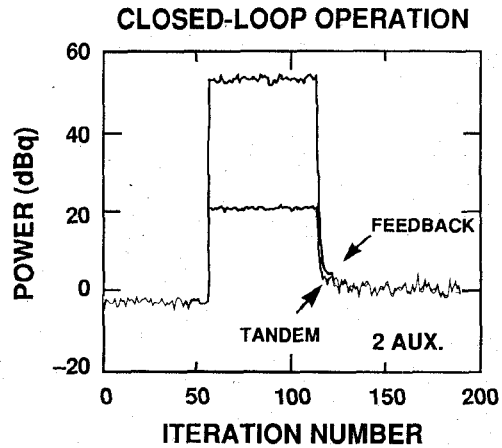


Fig. 16. Measured adaptive cancellation of a dispersive jamming signal with the four-channel nulling receiver operating in the closed-loop modes. An improvement in the dynamic range with closed-loop operation allows a larger cancellation compared with the feedforward mode (Fig. 15).

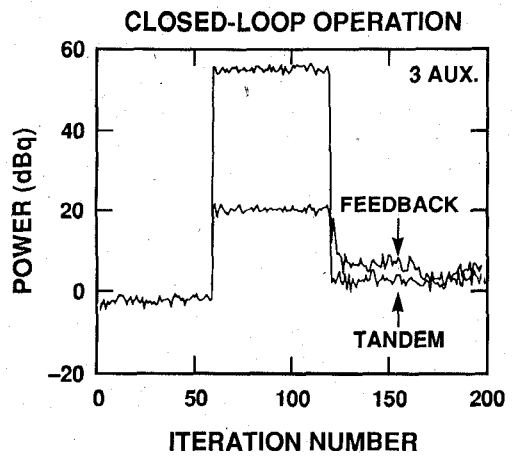


Fig. 17. Measured adaptive cancellation of a nondispersive jamming signal with the four-channel nulling receiver operating in the closed-loop modes. Notice the improved convergence of the tandem mode compared with the feedback mode. Convergence is achieved in effectively one iteration.

The four-channel experimental receiver routinely achieves 50 dB adaptive cancellation over a 1 MHz bandwidth in the all-digital feedforward mode. In this mode, performance is apparently limited by the useful dynamic range of the A/D converters. The hybrid feedback mode yields superior performance for perhaps two reasons. First, a somewhat higher interference level can be tolerated without causing saturation in the adapted output. Second, the subranging A/D converters in the experimental receiver generate less spurious noise when operated well below full scale range. Thus, for adaptive nulling purposes, the feedback mode exhibits both a larger dynamic range and a lower effective noise figure than the feedforward mode. Although the response of the feedback mode has been shown to suffer when the digital (SMI) weights behave erratically, the tandem mode has proven capable of restoring essentially instantaneous convergence.

## References

[1] I. S. Reed, J. D. Mallett, and L. E. Brennan, "Rapid convergence rate in adaptive arrays," *IEEE Trans. Aerosp. Electron. Syst.*, vol. AES-10, pp. 853–863, Nov. 1974.

[2] L. L. Horowitz, H. Blatt, W. G. Brodsky, and K. D. Senne, "Controlling adaptive antenna arrays with the sample matrix inversion algorithm," *IEEE Trans. Aerosp. Electron. Syst.*, vol. AES-15, pp. 840–848, Nov. 1979.

[3] C. L. Lawson and R. J. Hanson, *Solving Least Squares Problems*. Englewood Cliffs, NJ: Prentice-Hall, 1974.

[4] W. F. Gabriel, "Adaptive Arrays—An Introduction," *Proc. IEEE*, vol. 64, pp. 239–272, Feb. 1976.

[5] S. C. Pohlig, "Hybrid adaptive feedback nulling in the presence of channel mismatch," in *Proc. 1988 ICASSP* (New York, NY), Apr. 11–14, 1988, pp. 1588–1591.

[6] R. A. Monzingo and T. W. Miller, *Introduction to Adaptive Arrays*. New York: Wiley, 1980.

[7] R. T. Compton, Jr., *Adaptive Antennas, Concepts and Performance*. Englewood Cliffs, NJ: Prentice-Hall, 1988.

[8] J. R. Johnson, F. G. Willwerth, H. M. Aumann, and A. J. Fenn, "Receiver channel equalization for adaptive antennas: Experimental results," in *1990 IEEE AP-S Symp. Dig.*, 1990, pp. 194–197.

[9] L. L. Horowitz, "Convergence rate of the extended SMI algorithm for narrowband adaptive arrays," *IEEE Trans. Aerosp. Electron. Syst.*, vol. AES-16, pp. 738–740, Sept. 1980.

[10] G. H. Golub and C. F. Van Loan, *Matrix Computations*. Baltimore, MD: Johns Hopkins University Press, 1983.

[11] L. L. Horowitz, H. Blatt, W. G. Brodsky, and K. D. Senne, "Implementation of the sample matrix inversion algorithm for controlling adaptive antenna arrays," in *ELECTRO 1979 Proc.*, Apr. 24–26, 1979.

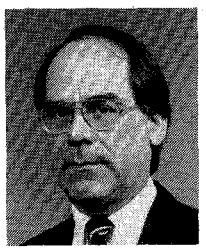

**J. Russell Johnson** received the S.B., S.M., and E.E. degrees from the Massachusetts Institute of Technology in 1966, 1970, and 1971, respectively, all in electrical engineering.

Mr. Johnson is a member of Eta Kappa Nu and Tau Beta Pi.

In 1971 he joined the staff at M.I.T. Lincoln Laboratory, where he has been involved in various radar applications, including adaptive clutter cancellation and precision direction-finding. His current interests include adaptive nulling and high-resolution spectral estimation.

**Alan J. Fenn** (S'74–M'79–SM'87) received the B.S. degree in electrical engineering from the University of Illinois, Chicago Circle Campus, in 1974. In 1976 and 1978, he received the M.S. and Ph.D. degrees, respectively, in electrical engineering from the Ohio State University, Columbus.

From 1974 to 1978, he was a Graduate Research Associate at the Ohio State University ElectroScience Laboratory. He was a Senior Engineer at Martin Marietta Aerospace, Denver, CO, from 1978 to 1981, where he was involved in broad-band antenna research and development. In 1981 he became a Staff Member at the Massachusetts Institute of Technology Lincoln Laboratory. He is in the space radar technology group, in which his research has involved phased array antenna design, adaptive nulling studies, and antenna and radar cross section measurements.

Dr. Fenn was a corecipient of the IEEE Antennas and Propagation Society's H. A. Wheeler Applications Prize Paper Award for 1990. He is currently an associate editor in the area of adaptive arrays for the IEEE TRANSACTIONS ON ANTENNAS AND PROPAGATION.

**Herbert M. Aumann** (S'64–M'67) received the B.S. degree in electrical engineering from the University of Idaho in 1965, the M.S. degree from Colorado State University in 1967, and the Ph.D. degree from the University of Wisconsin in 1973.

From 1967 to 1969, he was an instructor in the Department of Electrical Engineering at the University of Wisconsin. In 1973, he joined the Massachusetts Institute of Technology Lincoln Laboratory, working in various areas of radar signal processing. He is currently involved in space-based radar technology development.

Dr. Aumann was a corecipient of the IEEE Antennas and Propagation Society's H.A. Wheeler Applications Prize Paper Award for 1990.

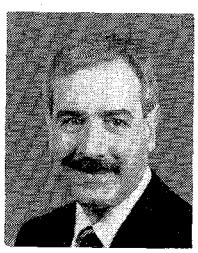

**Frank G. Willwerth** received the B.S. degree in electrical engineering from Tufts University in 1966, and subsequently did graduate work at Tufts University and at the Massachusetts Institute of Technology.

From 1966 to 1968, he was with Sylvania Electric Company, where he was engaged in microwave integrated circuit development. In 1968, he joined the Massachusetts Institute of Technology Lincoln Laboratory, where he is presently a staff member in the space radar technology group. His research has involved antenna design, near-field measurements, and adaptive nulling receiver design.

Mr. Willwerth was a corecipient of the IEEE Antennas and Propagation Society's H.A. Wheeler Applications Prize Paper Award for 1990.